

Flux penetration, matching effect, and hysteresis in homogeneous superconducting films

C. C. de Souza Silva, Leonardo R. E. Cabral, and J. Albino Aguiar

Lab. de Supercondutividade, Departamento de Física, Universidade Federal de Pernambuco, 50670-901 Recife, PE, Brazil

(Received 30 November 2000; published 15 March 2001)

The vortex dynamics in homogeneous superconducting films of arbitrary thickness under parallel magnetic field is studied. The strong surface effects in these systems are correctly taken into account by expressing the energy of the in-plane vortices in London background. A Langevin algorithm simulates the flux penetration and dynamical evolution of the vortices as the external field is slowly cycled. The numerical results show that the vortex lattice consists of linear chains of vortices parallel to the film surfaces and undergoes transitions involving formation or destruction of one chain, even for films with thickness greater than the penetration depth. In addition, the magnetization curve is irreversible and presents some similarities with Clem's model for surface pinning.

DOI: 10.1103/PhysRevB.63.134526

PACS number(s): 74.60.Ge, 74.25.Ha, 74.60.Ec, 74.76.-w

I. INTRODUCTION

In a type-II superconducting specimen the magnetic flux penetrates in the form of flux tubes generated by supercurrent vortices. For finite samples, the vortices nucleate at the surfaces and are pulled to the interior by the shielding supercurrents. Conversely, close to the sample edges, a vortex is strongly attracted by the superconductor-vacuum interface. These two competing interactions give rise to a surface barrier in the potential energy that delays the incursion of vortices towards the sample interior.^{1,2} When the external magnetic field is applied parallel to the surfaces, this energy barrier traps the vortices in such a way to result in an irreversible field-dependent magnetization curve $M(H)$, leading to finite critical currents even for homogeneous samples.^{3,4} Many aspects of vortex dynamics in superconducting crystals and films, such as creep phenomena,⁴ current induced ordering,^{5,6} dynamic instabilities and memory effects,⁶ are strongly influenced by the surface barriers.

Additional features of the magnetization curves come up when at least one of the sample dimensions is comparable to its characteristic penetration depth λ . For films with thickness $D \leq \lambda$ it was observed, both theoretically⁷⁻¹⁰ and experimentally,¹⁰⁻¹² that the $M(H)$ curves under parallel magnetic field exhibit peaks corresponding to sudden rearrangements in the vortex lattice (VL). Numerical minimization of the Gibbs free energy⁸⁻¹⁰ has shown that the vortices form a linear chain in the equatorial plane of the film when the external field is increased just above the corresponding lower critical field $H_{c1}(D)$. For a higher field value the competition between the repulsive vortex-vortex and vortex-surface interactions results in a buckling of the chain. As the field is further increased, new chains, one by one, are added in the VL. These transitions from n to $n+1$ chains occur in specific field values and are visible as peaks in the equilibrium $M(H)$ curve. The resulting equilibrium VL, as predicted in Ref. 13, is very close to a triangular lattice. Recently¹² we have found that when the surface barrier to vortex entry is considered the resulting metastable VL is distorted from the equilibrium one and the matching fields are history dependent.

In the present paper we investigate the behavior of the

in-plane VL in superconducting films of arbitrary thickness. We numerically simulate the penetration and dynamical evolution of the vortices as an external magnetic field H parallel to the film is slowly cycled at constant sweep rate. The key differences from this work to previous studies on this geometry⁸⁻¹⁰ are that our simulations are dynamical, following a Langevin dynamics algorithm, and films with thickness $D > \lambda$ are also considered. Two main results arise from the simulations. First, rearrangements in the vortex lattice leading to a change in the number of linear chains by one unity are present in all films studied, independently of their thickness. These rearrangements are seen as peaks in the irreversible $M(H)$ curves and in the VL ordering. Second, the magnetization of thick films is close to zero all over the descending branch of $M(H)$ curve. This provides evidence for Clem's macroscopic model for surface pinning³ where the vortices were predicted to exit the sample whenever the external field satisfied $H(B) \approx B$.

II. LONDON THEORY

We model a transversal section (xy plane) of an infinite type-II superconducting film of arbitrary thickness D (inset in Fig. 1). Periodic boundary conditions are considered in the y direction, with periodicity large enough (up to $L_y = 80\lambda$) to guarantee vanishing size effects. An external magnetic field H is applied parallel to the film surfaces (on the z axis) and the vortices are assumed to be straight and aligned with the field direction. Accordingly, we use two-dimensional London theory to determine the energy per unit length of an arbitrary distribution of stiff vortices:

$$\begin{aligned} \mathcal{E}_v = & \epsilon \sum_{i \neq j}^N \sum_{m=1}^{\infty} \frac{e^{-\alpha_m |\tilde{y}_i - \tilde{y}_j|}}{\alpha_m} \sin\left(\frac{m\pi\tilde{x}_i}{\tilde{D}}\right) \sin\left(\frac{m\pi\tilde{x}_j}{\tilde{D}}\right) \\ & + \phi_0 H \sum_{i=1}^N \left[\frac{\cosh(\tilde{x}_i - \tilde{D}/2)}{\cosh \tilde{D}/2} - 1 \right] \\ & + \epsilon \sum_{i=1}^N \sum_{m=1}^{\infty} \frac{e^{-\alpha_m \tilde{\xi}}}{\alpha_m} \sin^2\left(\frac{m\pi\tilde{x}_i}{\tilde{D}}\right), \end{aligned} \quad (1)$$

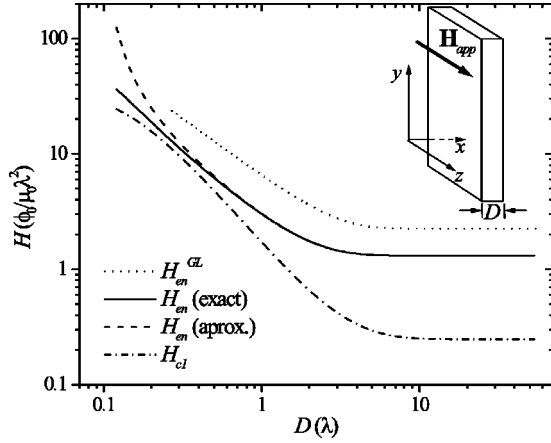


FIG. 1. Thickness dependence of the penetration field $H_{en}(D)$ as calculated by Eq. (2) (solid line) and Eq. (3) (dash), $H_{en}^{GL}(D)$, numerically calculated from Eq. (11) of Ref. 13 (dot), and the first critical field $H_{c1}(D)$ as calculated by the global minimum condition (dash-dot), for $\xi = 0.05\lambda$. Inset: film geometry and coordinate system.

where $\alpha_m = \sqrt{1 + (m\pi\lambda/D)^2}$, $\epsilon = \phi_0^2/2\mu_0\lambda D$, $\phi_0 = h/2e$ is the fluxoid quantum, μ_0 is the vacuum permeability and ξ is the coherence length. The tilde above length quantities means normalization by λ . The above equation was obtained in the spirit of Sardella *et al.* calculations,⁸ i.e., using the Green's-function method to solve the two-dimensional (2D) London equation for the local magnetic induction $b(x, y)$. The first term of Eq. (1) stands for the interaction between every pair of vortices inside the sample. The second one is the repulsive interaction energy between each vortex with the Meissner screening currents (i.e., with the homogeneous solution of London equation). The condition that transverse currents are forbidden on the film surfaces and a suitable cutoff in the vortex self-interaction leads to the self-energy of the vortices (third term). This term is attractive and, together with the second one, forms the surface barrier.

In our model, the vortices are considered to nucleate inside the film at a distance ξ from one of the surfaces. (At smaller distances, London theory fails because of the depreciation of the superconducting order parameter near the surface.) The criterion for the vortex entrance is a force-balance condition, i.e., the first vortex enters the film when the Lorentz force due to the screening currents becomes greater than the self-force. The field value for which this balance is achieved is called the first entry field H_{en} . In the London background, using the above described entrance criterion, the normalized value of the entry field ($\tilde{H}_{en} = \mu_0\lambda^2 H_{en} / \phi_0$) for stiff vortices is expressed by

$$\tilde{H}_{en} = \frac{\pi}{2\tilde{D}^2} \frac{\cosh(\tilde{D}/2)}{\sinh(\tilde{D}/2 - \tilde{\xi})} \sum_{m=1}^{\infty} \frac{m}{\alpha_m} e^{-\alpha_m \tilde{\xi}} \sin\left(\frac{2m\pi\tilde{\xi}}{\tilde{D}}\right). \quad (2)$$

For small ξ/D values, the series in the above expression can be suitably replaced by an integral, which represents the modified Bessel function of the first kind K_1 . In this case, Eq. (2) can be expressed in the closed form:

$$\tilde{H}_{en}(\tilde{D} \gg \tilde{\xi}) = \frac{K_1(\sqrt{5}\tilde{\xi})}{\pi\sqrt{5}} \frac{\cosh(\tilde{D}/2)}{\sinh(\tilde{D}/2 - \tilde{\xi})}. \quad (3)$$

In the high- κ limit (small $\tilde{\xi}$), Eq. (3) provides a good approximation for films with thickness $D \gg \lambda$ (see Fig. 1). Another important feature of this expression is that in the bulk limit ($D \gg \lambda$) the entry field is close to the thermodynamic critical field H_c (as was also obtained by de Gennes² for a semi-infinite specimen using a similar entrance criterion) and is attained for films as thin as a few λ . For $\tilde{\xi} = 0.05$ (value adopted in all simulations), \tilde{H}_{en} is essentially constant (assuming the value 1.315) for films with $D \geq 8\lambda$.

To include the effect of the vortex core and the depreciation of the order parameter, de Gennes used one-dimensional Ginzburg-Landau theory¹⁴ and found an integral expression for the entry field H_{en}^{GL} of a film with arbitrary thickness [Eq. (11) of Ref. 14] for which the bulk limit is exactly H_c . However, for films with $D \gg \xi$, H_{en} (calculated in London background) has a similar thickness dependence and differs from H_{en}^{GL} by a numerical factor (see Fig. 1). Furthermore, as we shall discuss later, the true value for the entry field is smeared out by surface imperfections, vortex deformation and every kind of fluctuations. For this reason, we will concentrate on the qualitative behavior of the macroscopic quantities and the effect of the surface barrier on the vortex dynamics rather than numerical values.

In contrast with the above dynamical process, for thermodynamic equilibrium calculations a vortex is allowed to enter the sample as soon as a global minimum in the Gibbs free energy appears, i.e., the vortices do not have to overcome the surface barrier. As it is well known, this condition defines the first thermodynamic critical field $H_{c1}(D)$, which is smaller than $H_{en}(D)$. As shown by Pethukov and Chechetkin,¹⁵ the activation energy for the nucleation and further penetration of vortices in the field region $H_{c1} < H < H_{en}$ is five orders of magnitude greater than kT . Namely penetration of vortices below H_{en} is almost impossible. Nevertheless, in real samples H_{en} may be strongly affected by surface imperfections, which produces leaks for the passage of vortices through the surface barrier, leading to a H_{en} value between $H_{c1}(D)$ and the perfect-surface value. We believe, however, that this suppression of H_{en} would not significantly affect the field dependence of the VL dynamics.

III. LANGEVIN DYNAMICS AND NUMERICAL DETAILS

To a good approximation, vortices in most of classic and high- T_c superconductors move as massless particles embedded in a dissipative background. For this reason, we simulate the dynamical evolution of a vortex that has fulfilled the force balance condition by solving its overdamped Langevin equations of motion,

$$\eta \frac{d\mathbf{x}_k}{dt} = -\nabla_k \mathcal{E}_v - \mathbf{R}_k(t). \quad (4)$$

Here, η is the friction coefficient, \mathbf{x}_k is the position of vortex k in the xy plane and ∇_k is the gradient operator with respect

to vortex k position. $\mathbf{R}_k(t)$ is a stochastic force which is related to the temperature by the fluctuation-dissipation theorem. In our simulations we assume this temperature to be very low (as compared to the VL melting temperature) and to have been attained after a zero-field cooling process. In this way we can neglect relaxation through the surface barriers towards equilibrium and concentrate on stationary metastable states.

We simulate a magnetization measurement as an external field H is slowly looped. Every time step a vortex is placed at each film surface in random y positions and attempted to enter the sample. Interactions with other vortices already accepted in the system, if any, are incorporated into the force-balance condition. Equation (4) is then solved at each time step for every vortex inside the sample. Past a fixed number Δt of time steps the external field is increased (or decreased) by a small amount ΔH . The sweep rate $\Delta H/\Delta t$ is carefully chosen to permit a considerably stable VL configuration spending minimum computing time. Snapshots of the VL configurations are periodically recorded all over the magnetization curves. For each VL record we use an algorithm based on Delauney triangulation to find the natural neighbors of each vortex and compute the sixfold coordination number probability, $\mathcal{P}_6(H)$. For the systems studied, this quantity is a measure of the VL ordering.

IV. RESULTS AND DISCUSSION

The as calculated $M(H)$ for films with thickness ranging from λ to 8λ are plotted in Fig. 2. All of them are characterized by hysteresis with the presence of extra peaks at both ascendant and descendant curve branches. Records of the VL configuration (some of them screened in Fig. 3) show that these peaks correspond to rearrangements in the VL in which the number of chains change by one unity to perfectly match the energy profile. The field values H_n where these rearrangements take place are usually called matching fields, (n is the number of vortex chains *after* rearrangement). In Fig. 4 we plot the thickness dependence of some matching fields of the ascendant branch. These curves represent the transitions between neighbors metastable states. Each transition is preceded by a disorder on the VL and followed by an ordered state. This fact is pointed up in the inset of Fig. 4 where we plot $\mathcal{P}_6(H)$, in ascendant field, for the 8λ film. (Note that only transitions resulting in three or more chains are observable because the vortices closer to the film surfaces have only three neighbors.)

Another important feature of this matching effect is its history dependent behavior. As the field is increasing a new chain is formed after each matching field. In the descendant branch, instead, a vortex chain is completely destroyed as the field is decreased below the corresponding H_n value. Nevertheless, as it is well illustrated by the dashed lines in Fig. 2, the values of H_n for the ascendant and descendant branches are quite different. Moreover, we may have the peculiar situation depicted in Fig. 3(d), where a transition from 10 to 11 vortex chains, which would be expected to occur only in the ascendant branch, take place as the field is decreasing from its maximum value.

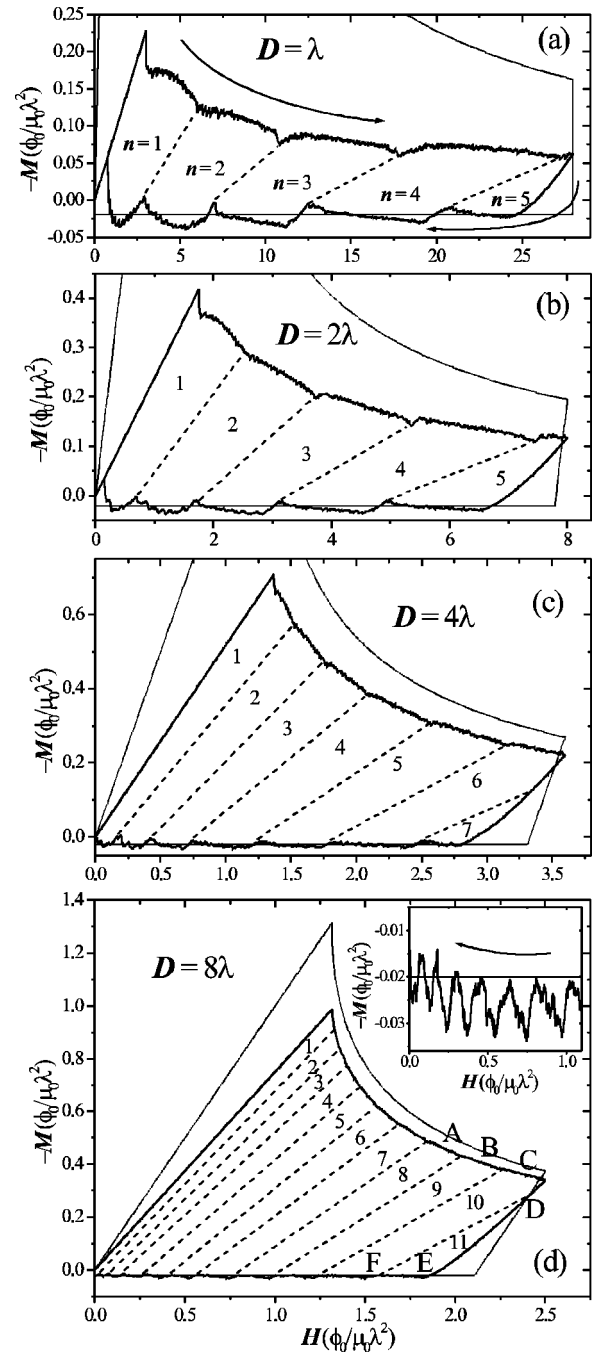


FIG. 2. Magnetization curves (thick solid lines) calculated for thin homogeneous films with thickness $D = \lambda$ (a), 2λ (b), 4λ (c), and 8λ (d). The dashed straight lines are just guides for better visualization of the transitions between successive chain arrangements and the numbers between them indicate the number of chains of the VL. The thin solid lines correspond to the magnetization loops as obtained by the macroscopic model of Ref. 3.

The asymmetry of the magnetization curve is a result of the different circumstances in which a vortex enters or exits the sample. In increasing field the surface barrier develops a vortex free region within a distance x_{vf} from the film surfaces. This length is considerably greater than the lattice parameter a of the VL (see Fig. 3) and its field dependence

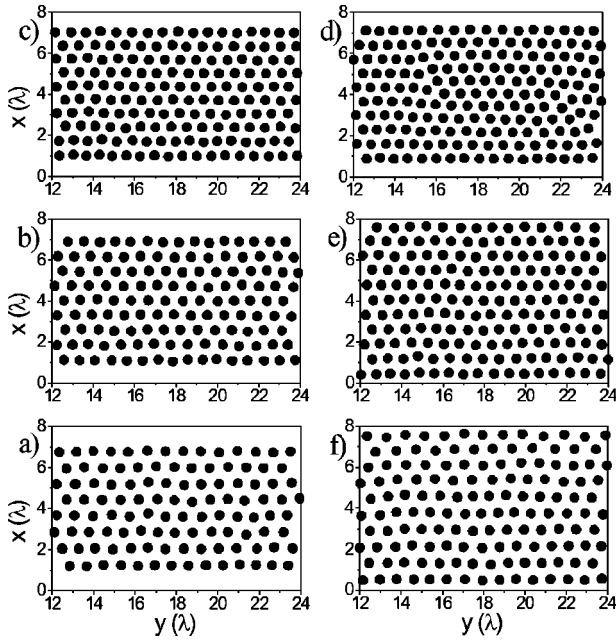


FIG. 3. Snapshots of the vortex lattice in a slice of the 8λ film for the points A, B, C, D, E, and F indicated in Fig. 1(d). The external field values, in units of $\phi_0/\mu_0\lambda^2$, are, respectively: 1.9 (a), 2.2 (b), and 2.4 (c) in ascendant field, and 2.4 (c), 1.8 (e), and 1.52 (f) in descendant field.

strongly affects the magnetization. In contrast, for decreasing field, x_{vf} will monotonically decrease until it reaches a small value (smaller than a) from which vortices dramatically approach the film surfaces and start to leave the sample. At this moment, the macroscopic magnetic induction comes close to the external field. In the interval of the decreasing branch where no flux exits, the effective area of the VL in the film cross section enlarges, which makes possible the formation of a new vortex chain without any change in the number of vortices [e.g., Fig. 3(d)]. Clem has formerly described these vortex free regions and its implications to the $M(H)$ curve by using locally averaged fields and currents in a bulk sample.⁵ Nevertheless, his model does not predict the structural transitions in the VL. Actually, the shape of the $M(H)$ loops we derive for the thicker films, disregarding the extra peaks, is quite similar to the curves obtained by the macroscopic model where the ascendant branch has the simple form of a hyperbola,

$$M(H) = H - \sqrt{H^2 - H_{en}^2}, \quad (5)$$

and the descendent branch assumes the constant value $1/16\pi \approx 0.020$ (see Fig. 2). For films with thickness comparable to the penetration depth, the Meissner field completely

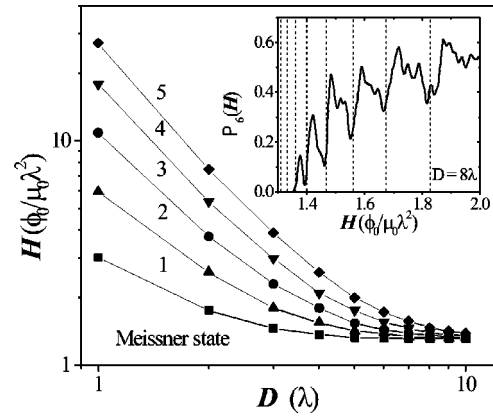


FIG. 4. Magnetic-field film thickness diagram for ascendant field showing several metastable states for the vortex lattice. The data corresponds to the thickness dependent matching fields $H_1 \equiv H_{en}$ (squares), H_2 (up triangles), H_3 (circles), H_4 (down triangles), and H_5 (diamonds), obtained in the simulations. Inset: six-fold coordination probability for ascendant field for the 8λ film.

penetrates the sample diminishing the magnetization response. For this reason, Eq. (5) does not hold unless the condition $D \gg \lambda$ is satisfied. However, the descendant branch, even for the thinnest film studied ($D = \lambda$), oscillates about the value 0.02. Namely, the entrance of a vortex line when other vortices are present is strongly thickness dependent whereas its exit is not.

V. CONCLUSIONS

In summary, we have simulated a magnetization loop experiment for an infinite homogeneous superconducting film under a parallel magnetic field. We have shown that the in plane VL goes through transitions with the formation or destruction of a vortex chain. These rearrangements are irreversible and are visible as a series of extra peaks in the magnetization curve. The suppression of the sixfold coordination probability near the matching fields is also a striking signature of the VL transitions. We also demonstrated that the overall magnetization loop for thick films draws near the bulk limit obtained by usually adopted macroscopic models³ for surface pinning. We would like to stress that the main features of the magnetization curves obtained here should be experimentally accessible for typical values of the interest parameters.

ACKNOWLEDGMENTS

The authors acknowledge G. M. Carneiro for stimulating discussions. This work was sponsored by the Brazilian Agencies CNPq, FACEPE, and FINEP.

¹C. P. Bean and J. D. Livingston, Phys. Rev. Lett. **12**, 14 (1964).

²P. G. de Gennes, *Superconductivity of Metals and Alloys* (Benjamin, New York, 1966), Chap. 3, p. 76.

³J. R. Clem, in *Low Temperature Physics*, edited by K. D. Tim-

merhaus, W. J. O'Sullivan, and E. F. Hammel (Plenum, New York, 1974), Vol. 3, p. 102.

⁴L. Burlachkov, Phys. Rev. B **47**, 8056 (1993).

⁵S. N. Gordeev, P. A. J. de Groot, M. Oussena, A. V. Volkozub, S.

- Pinfold, R. Langan, R. Gagnon, and L. Taillefer, *Nature (London)* **385**, 324 (1997).
- ⁶Y. Paltiel, E. Zeldov, Y. N. Myasoedov, H. Shtrikman, S. Bhattacharya, M. J. Higgins, Z. L. Xiao, E. Y. Andrei, P. L. Gamel, and D. J. Bishop, *Nature (London)* **403**, 398 (2000), and references therein.
- ⁷C. C. de Souza Silva and J. Albino Aguiar, *Physica C* (to be published).
- ⁸E. Sardella, M. M. Doria, and P. R. S. Netto, *Phys. Rev. B* **60**, 13 158 (2000).
- ⁹G. Carneiro, *Phys. Rev. B* **57**, 6077 (1998).
- ¹⁰S. H. Brongersma, E. Verweij, N. J. Koeman, D. G. de Groot, R. Griessen, and B. I. Ivlev, *Phys. Rev. Lett.* **71**, 2319 (1993).
- ¹¹M. Ziese, P. Esquinazi, P. Wagner, H. Adrian, S. H. Brongersma, and R. Griessen, *Phys. Rev. B* **53**, 8658 (1996).
- ¹²C. C. de Souza Silva and J. Albino Aguiar, *Physica B* **284**, 634 (2000).
- ¹³V. V. Schmidt, *Zh. Éksp. Teor. Fiz.* **57**, 2095 (1969) [*Sov. Phys. JETP* **30**, 1137 (1970)]; **61**, 398 (1971) [**34**, 211 (1972)]; A. I. Rusinov and G. S. Mkrtchan, *ibid.* **61**, 773 (1971) [**34**, 413 (1972)].
- ¹⁴P. G. de Gennes, *Solid State Commun.* **3**, 127 (1965).
- ¹⁵B. V. Petukhov and V. R. Chechetkin, *Zh. Éksp. Teor. Fiz.* **65**, 1653 (1973) [*Sov. Phys. JETP* **38**, 827 (1974)].